Low-Cost Sensors based Multi-sensor Data Fusion Techniques for RPAS Navigation and Guidance

Francesco Cappello, Subramanian Ramasamy, Roberto Sabatini and Jing Liu
School of Aerospace, Mechanical and Manufacturing Engineering
RMIT University, Melbourne, VIC 3000, Australia
roberto.sabatini@rmit.edu.au

***Abstract*—In order for Remotely Piloted Aircraft Systems (RPAS) to coexist seamlessly with manned aircraft in non-segregated airspace, enhanced navigational capabilities are essential to meet the Required Navigational Performance (RNP) levels in all flight phases. A Multi-Sensor Data Fusion (MSDF) framework is adopted to improve the navigation capabilities of an integrated Navigation and Guidance System (NGS) designed for small-sized RPAS. The MSDF architecture includes low-cost and low weight/volume navigation sensors suitable for various classes of RPAS. The selected sensors include Global Navigation Satellite Systems (GNSS), Micro-Electro-Mechanical System (MEMS) based Inertial Measurement Unit (IMU) and Vision Based Sensors (VBS). A loosely integrated navigation architecture is presented where an Unscented Kalman Filter (UKF) is used to combine the navigation sensor measurements. The presented UKF based VBS-INS-GNSS-ADM (U-VIGA) architecture is an evolution of previous research performed on Extended Kalman Filter (EKF) based VBS-INS-GNSS (E-VIGA) systems. An Aircraft Dynamics Model (ADM) is adopted as a virtual sensor and acts as a knowledge-based module providing additional position and attitude information, which is pre-processed by an additional/local UKF. The E-VIGA and U-VIGA performances are evaluated in a small RPAS integration scheme (i.e., AEROSONDE RPAS platform) by exploring a representative cross-section of this RPAS operational flight envelope. The position and attitude accuracy comparison shows that the E-VIGA and U-VIGA systems fulfill the relevant RNP criteria, including precision approach in CAT-II. A novel Human Machine Interface (HMI) architecture is also presented, whose design takes into consideration the coordination tasks of multiple human operators. In addition, the interface scheme incorporates the human operator as an integral part of the control loop providing a higher level of situational awareness.**

Keywords*—*Remotely Piloted Aircraft Systems; Aircraft Dynamics Model; Unscented Kalman Filter; Low-cost sensors; Navigation and Guidance System; Multi-sensor Data Fusion; Human Machine Interface.

I. INTRODUCTION

The development and operation of Remotely Piloted Aircraft Systems (RPAS) has rapidly expanded in recent years. Small- to medium-size RPAS are being proposed as alternatives to manned aircraft in an increasing number of civil, military and research applications especially in Dull, Dirty and Dangerous (D3) roles [1]. In particular, small RPAS have the ability of performing tasks with higher maneuverability and longer endurance as well as posing less risk to human lives and nature [2]. A major developmental challenge for RPAS is their integration into non-segregated airspace. Currently operations are mostly segregated and the challenges involved with their integration into commercial airspace are currently being addressed through various operational and technological developments. These developments are focusing on enhanced Communication, Navigation, Surveillance, Air Traffic Management and Avionics (CNS+A) systems, Detect-and-Avoid (DAA) solutions and airworthiness block upgrades as depicted in Fig. 1 [3].

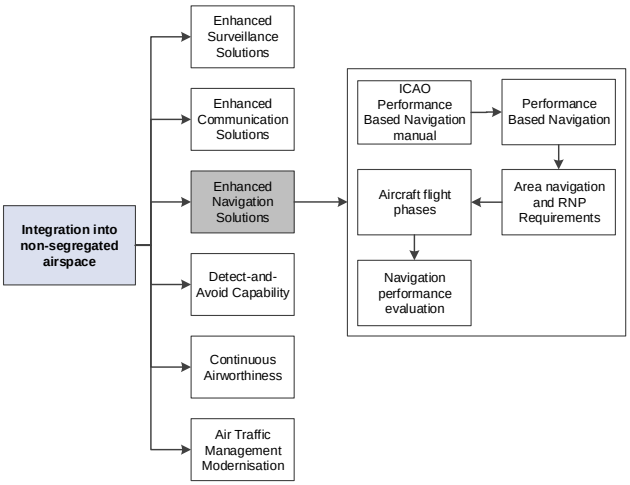

Fig. 1. RPAS Integration requirements.

Enhanced navigation systems must meet Performance Based Navigation (PBN) requirements in order to increase integration harmonization. PBN represents a fundamental shift from sensor-based to performance-based navigation [2]. The advantages of the PBN approach over the sensor-specific method of developing airspace and obstacle clearance criteria [2] include: a reduction in work required to maintain sensor-specific routed and procedures (and their associated costs); avoiding the need for developing sensor-specific operations with each new evolution of navigation systems (which would be cost prohibitive); a more efficient use of airspace (route placement, fuel efficiency and noise

abatement). These advantages facilitate the operational approval process by providing a limited set of navigation specifications intended for global use. In terms of RPAS airworthiness, operations will have to be equivalent to manned aircraft. In addition they will have to prove to be as safe as current manned operations and have to meet the Required Navigational Performance (RNP) levels through all flight phases [3, 10, 11]. To achieve global interoperability of RPAS and manned aircraft a guiding framework for technology upgrades is envisaged by the International Civil Aviation Organization (ICAO) as part of Aviation System Block Upgrades (ASBU) [3]. Basic procedures and functions which will initiate integration include DAA functions. Both Line-of-Sight (LOS) and Beyond-Line-of-Sight (BLOS) secure and safe communication links are essential for the RPAS to maintain continuous contact with the Ground Control Station (GCS). Significant outcomes are also expected from large-scale and regional ATM modernisation programmes including Single European Sky ATM Research (SESAR) and Next Generation Air Transportation System (NextGen). In line with the identified CNS+A evolutions, a key goal for seamless global air traffic management is implementing advanced digital and satellite systems together with other technologies that increase the levels of automation in communications, navigation, and surveillance tasks. Automatic Dependent Surveillance-Broadcast (ADS-B) and Traffic Collision Avoidance System (TCAS) can be used to provide cooperative DAA functions. High-integrity airborne and ground-based integrated Navigation and Guidance Systems (NGS) that include fail-safe architecture designs are required to meet the RNP requirements in all flight phases. Another important goal aspect is to develop novel forms of Human Machine Interface (HMI) suitable for RPAS operations in all classes of airspace. Fig. 2 illustrates the RPAS main components, including the Command and Control (C^2) link between the Remote Pilot Aircraft (RPA) and the Ground Control Station (GCS). Fig. 3 depicts the information interchanges between the RPAS pilot and the RPA to accomplish a planned mission.

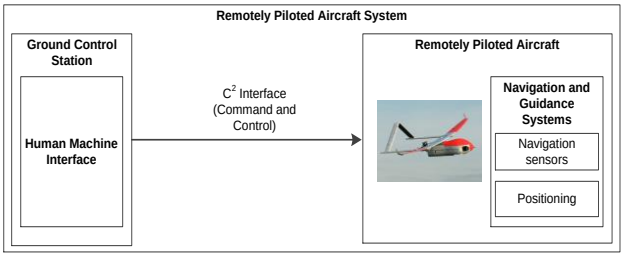

Fig. 2. RPAS requirements.

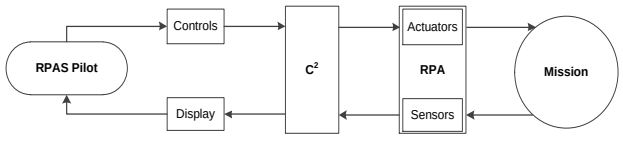

Fig. 3. Human supervisory RPAS cpntrol loop.

II. Multi–Sensor Data Fusion

Our previous research activities [24-30] on NGS for small-medium size RPAS presented the various sensor options, data fusion methods and test activities performed to evaluate the performance of the overall system. The selection of suitable navigation sensors is based on the requirements for low-cost, low-weight/volume sensors capable of providing the required levels of performance for small-to-medium size RPAS in all flight phases. Sensor candidates include Global Navigation Satellite System (GNSS) and Micro-Electro-Mechanical System (MEMS) based Inertial Measuring Unit (IMU), which provide a highly synergistic combination and are capable of providing enhanced navigation and inertial reference performance and dissimilarity for fault tolerance and anti-jamming [31]. The main objective is to design a compact, lightweight and relatively inexpensive system capable of providing the required navigation performance in all phases of flight of a small RPAS, with a special focus on precision approach and landing, where Vision Based Navigation (VBN) techniques can be fully exploited in a multisensory integrated architecture. sensors are also used for precision approach and landing (i.e., the most demanding and potentially safety-critical flight phase). An Aircraft Dynamics Model (ADM) can be used as a virtual sensor (essentially a knowledge-based module) and augments the navigation state vector [32, 33, 27]. When processed with suitable optimal estimation techniques, the ADM predicts the RPAS flight dynamics (aircraft trajectory and attitude motion). This approach allows a reduction of cost, weight/volume and support requirements and, with the appropriate combination of sensors and integration algorithms, gives increased accuracy, continuity, availability and integrity to the overall system [5, 6]. In this paper, we propose an integrated NGS approach employing three state-of-the-art physical sensors: MEMS-IMU, GNSS and VBN sensors, as well as augmentation from ADM [5-7]. In particular, the ADM is used to compensate for the MEMS-IMU sensor shortcomings experienced in high-dynamics attitude determination tasks. Position, velocity and attitude measurements are obtained from GNSS. MEMS-based INS provides position and velocity data while attitude measurements are also obtained both from INS and VBN sensors. Multi-Sensor Data Fusion (MSDF) techniques are adopted for an optimal integration of the various sources of information, resulting in deriving inferences that are not feasible from a single sensor or source [12]. Techniques for data fusion of low-cost sensors range from position estimation such as Kalman filtering to more advanced methods such as fuzzy expert systems [13] and neural networks, which implement Kalman Filtering methods including Extended Kalman Filter (EKF) [14] and particle filter [15]. The EKF has been at the forefront of applied optimal estimation for the past 30 years [16]. However, recent advancements in computation power have led to the rise of a number of additional techniques for data fusion such as the Cubature Kalman Filter (CKF) [17], Central Difference Kalman Filter (CDKF) [18, 19], Square Root-Unscented Kalman Filter (SR-UKF) [16] and Particle Filter (PF) [20]. Recently, the adoption of UKF has overshadowed the EKF in many real-time applications,

thanks to the quicker convergence rate and handling of nonlinearities in real-time. Previous research showed that the UKF is more accurate and robust than EKF in several applications due to its superior convergence characteristics [21]. The UKF is a recursive state estimator and is based on the Unscented Transform (UT) process, which is a method to approximate the mean and covariance of a random variable undergoing a nonlinear transformation [22]. The UKF uses sigma points to evaluate the statistics of a nonlinear transformed random variable. The UKF captures the posterior mean and covariance accurately to the 3rd order (Taylor series expansion) for any nonlinearity [23]. The data provided by all sensors are blended using an UKF. A loosely coupled integration method is implemented, which approach supports integration of Commercial Off-The-Shelf (COTS) and low-cost navigation sensors. The advantages of adopting an UKF are:

- Eliminates the need of Jacobeans or Hessians.
- Ease of higher order approximations.
- Better performance in non-linear problems.
- More relevance to real-life problems and conditions.
- Increased ADM vertical and horizontal validity/operational time.

The UKF is generally classified into [13]:

- Additive UKF that reduces the order and subsequently the number of mathematical calculations required in each iteration, without using the augmented states of the traditional UKF. This filter is computationally efficient and hence adopted in real-time systems.
- Square-root UKF that is used to prevent numerical instabilities to which the algorithm is exposed, being necessary to conserve the covariance matrix of the state errors as semi-defined positive.
- Spherical complex UKF that utilizes an alternative criterion for selecting a minimum set of sigma points. This variant overcomes a key drawback of the UKF, which is the relative poor execution speed when compared to EKF.

The UT process is based on a sequence of tasks: computation of a set of sigma points, assignment of weights to each sigma point, transformation of the sigma point through a nonlinear function and computation of the Gaussian weighted points. As shown in Fig. 4, sigma points are obtained based on mean and covariance values.

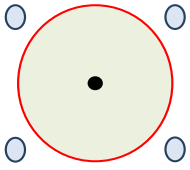

Sigma Points: Blue
Mean: Black
Covariance: Red circumference

Fig. 4. Calculated sigma points.

The UT process then transforms the sigma points to a new set as depicted below in Fig. 5.

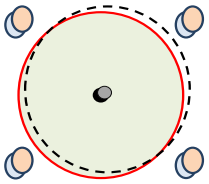

Sigma Points: Blue
Mean: Black
Covariance: Red circumference
Transformed Sigma Points: Orange
Mean obtained after UT: Grey
UT covariance: Dotted line

Fig. 5. Transformed sigma points.

The following algorithm is used for state estimation [16]. Initialisation of the UKF is performed based on the process model equations given by:

$$\hat{x}_0 = m[x_0] \tag{1}$$

$$P_0 = m[(x_0 - \hat{x}_0)(x_0 - \hat{x}_0)^T] \tag{2}$$

where $\hat{x}_0$ is the initial state vector estimate, m is the mean or expected value, x_0 is the initial state vector, which incorporates the initial state of the ADM, P_0 is the initial state covariance matrix and T is the transposition of the matrix. The process model of the UKF is based upon a set of sigma points. The sigma points, χ_i are selected based on the mean and covariance of x_k. The multi-sensor data fusion architecture is based on a federated architecture. The process model is based on a set of sigma points, which are selectively chosen for improving the performance of the data fusion process. The sample value equations are given below:

$$\chi_0 = x_m \tag{3}$$

$$\chi_i = x_m + \left(\sqrt{(n+\kappa)P_{xx}}\right)_i \tag{4}$$

$$\chi_i = x_m - \left(\sqrt{(n+\kappa)P_{xx}}\right)_{i-n} \tag{5}$$

where χ is the initial mean of the sigma points (sample values), P_{xx} is the initial covariance matrix, m is the mean value, $i = 1, 2, \ldots, n$ is the index, κ is the integer scaling factor and n is the outer value. κ is introduced as a tuning parameter for the calculation of the sigma points. The algorithm is designed to sample the mean and covariance of an arbitrary function that satisfies its state variable and follows a normal distribution. The nonlinear function is applied to each sigma point, which in turn yields a cloud of transformed points and the statistics of the transformed points. Since the problem of statistical convergence is not a substantial drawback, higher order information about the distribution can be captured using only a very small number of points [19]. The UT process is described by introducing a random variable x (dimension n) and is assumed to be propagated through a nonlinear function, $f = g(x)$ and x is represented by the mean and covariance values. At the end of this process, a valid selection of sigma points is obtained. The transformed points are given a weighting known as sample weight that are given by:

$$W_{\mathrm{i}} = \frac{\kappa}{n+\kappa} \tag{6}$$

$$W_{i+1} = \frac{1}{2(n+\kappa)} \quad (7)$$

$$W_{i+n+1} = \frac{1}{2(n+\kappa)} \quad (8)$$

where W is the initial weight. The sample values attained from the measurements are fed into the UKF. In the equations above $\left(\sqrt{(n+\kappa)P_{xx}}\right)_i$ is equal to u_i which is a row vector. These values are obtained from the matrix $U^T U = (n+\kappa)P_x$, where κ is an arbitrary constant. The sigma points are obtained by [16]:

$$P_{k-1} = \{diag(P_{k-1})\}^T \quad (9)$$

$$\chi_{k-1} = \left[\hat{x}_{k-1} \;\; \hat{x}_{k-1} + \gamma\sqrt{P_{k-1}} \;\; \hat{x}_{k-1} - \gamma\sqrt{P_{k-1}}\right] \quad (10)$$

where P computes the diagonal of state covariance matrix and results in the lower triangular matrix of the state covariance matrix P and γ is the control parameter of the dispersion distance from the mean estimate in the computation of the sigma point matrix, χ. After the sigma points are calculated, a time update for each time step $k = 1, 2, \ldots,$ n is performed and is given by [16]:

$$\chi^*_{k|k-1} = fn[\chi_{k-1}, u_{k-1}] \quad (11)$$

$$\hat{x}_k^- = \sum_{i=0}^{2L} W_i^{(m)} \chi^*_{i,k|k-1} \quad (12)$$

$$P_k^- = \sum_{i=0}^{2L} W_i^{(C)} \left[\chi^*_{i,k|k-1} - \hat{x}_k^-\right]\left[\chi^*_{i,k|k-1} - \hat{x}_k^-\right]^T + R^v \quad (13)$$

$$^5\chi_{k|k-1} = \left[\hat{x}_k^- \;\; \hat{x}_k^- + \gamma\sqrt{P_k^-} \;\; \hat{x}_k^- - \gamma\sqrt{P_k^-}\right] \quad (14)$$

$$\mathcal{Y}_{k|k-1} = fn\left[\chi_{k|k-1}\right] \quad (15)$$

$$\hat{y}_k^- = \sum_{i=0}^{2L} W_i^{(m)} y_{i,k|k-1} \quad (16)$$

where χ_k represents the unobserved state of the system, u_k is a known exogenous input, W_i is a set of scalar weights that corresponds to each sigma point when it undergoes a nonlinear transformation at each iteration $i = 1, 2, \ldots, 2L$. R^v is the process noise covariance matrix, C in $W_i^{(C)}$ is the covariance and m in $W_i^{(m)}$ is the mean and L is the dimension of the augmented state vector. The measurement update equations are given by [16]:

$$P_{\tilde{y}_k\tilde{y}_k} = \sum_{i=0}^{2L} W_i^{(C)} \left[\mathcal{Y}_{i,k|k-1} - \hat{y}_k^-\right]\left[\mathcal{Y}_{i,k|k-1} - \hat{y}_k^-\right]^T + R^n \quad (17)$$

$$P_{x_k y_k} = \sum_{i=0}^{2L} W_i^{(C)} \left[\chi_{i,k|k-1} - \hat{x}_k^-\right]\left[\mathcal{Y}_{i,k|k-1} - \hat{y}_k^-\right]^T \quad (18)$$

$$\mathcal{K}_k = P_{x_k y_k} P^{-1}_{\tilde{y}_k\tilde{y}_k} \quad (19)$$

$$\hat{x}_k = \hat{x}_k^- + \mathcal{K}_k(y_k - \hat{y}_k^-) \quad (20)$$

$$P_k = P_k^- - \mathcal{K}_k P_{\tilde{y}_k\tilde{y}_k} \mathcal{K}_k^T \quad (21)$$

where R^n is the measurement noise covariance matrix [16]. The parameter $\mathcal{Y}$ is the nonlinear function used for propagation of the sigma points, x_k is the k^{th} component of the vector x, $\hat{x}$ is an estimate of the value of x, $\hat{x}_k(-)$ is a-priori estimate of x_n, conditioned on all priori measurements except the one at time t_k, $\hat{x}_k(+)$ is a-posteriori estimate of x_k, conditioned on all priori measurements at time t_k. The UKF calculates the new sigma points every time in the time update and hence it requires the computation of a matrix square-root of the state covariance. The generic algorithm of the UKF is illustrated in Fig. 6.

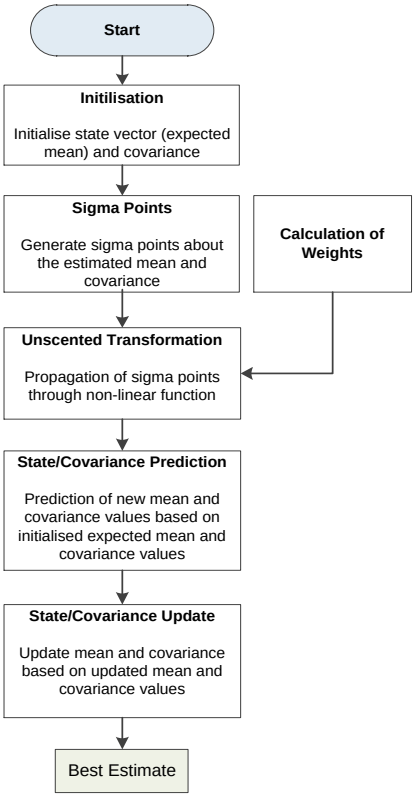

Fig. 6. Generic algorithm of the UKF.

A. *Aircraft Dynamics Model*

With reference to the implementation of the ADM, six Degrees of Freedom (6-DOF) geodetic nonlinear equations force and moment equations are listed below, describing the motion of the aircraft in the body frame G with:

- A velocity $V = [u\ v\ w]^T$ with regards to the inertial frame, expressed in the body frame G.
- An angular rates $w = [p\ q\ r]$

where u is the axial velocity, v is the lateral velocity and w is the normal velocity, p is the roll rate, q is the pitch rate and r is the yaw rate.

1) Forces Equations:

The equations describing the forces applied on the aircraft are described below. Gravitational forces act on the gravity center of the aircraft are given by:

$$(F_x)_{gravity} = -mg\sin\vartheta \quad (22)$$

$$\left(F_y\right)_{gravity} = mg\cos\vartheta\sin\varphi \quad (23)$$

$$(F_z)_{gravity} = mg\cos\vartheta\cos\varphi \quad (24)$$

where ϑ is pitch, φ is roll, ψ is yaw angle, G is acceleration due to gravity and M is mass of the RPAS. Similarly, propulsion forces are given by:

$$(F_x)_{engine} = T cos\epsilon \quad (25)$$

$$(F_y)_{engine} = 0 \quad (26)$$

$$(F_z)_{engine} = -T sin\epsilon \quad (27)$$

where T is thrust supplied by engines, ϵ is angle between the $X_b - axis$ and the mounted axis of the engines. The aerodynamic forces acting on the x, y and z axis are denoted as X, Y and Z respectively. The set of forces equations are given by:

$$m(\dot{u} + qw - rv) + u * \dot{m} = X - mgsin\vartheta + T cos\epsilon \quad (28)$$

$$m(\dot{v} + ru - pw) + v * \dot{m} = Y + mgcos\vartheta sin\varphi \quad (29)$$

$$m(\dot{w} + pw - qu) + w * \dot{m} = Z + mgcos\vartheta cos\varphi - T sin\epsilon \quad (30)$$

2) Moment equations:

The kinematic moments are expressed as:

$$H_x = pI_x - qI_{xy} - rI_{xz} \quad (31)$$

$$H_y = -pI_{xy} + qI_y - rI_{yz} \quad (32)$$

$$H_z = -pI_{xz} - qI_{yz} + rI_z \quad (33)$$

where:

$$I_x = \iiint y^2 + z^2 dm \; ; I_y = \iiint x^2 + z^2 dm \quad (34)$$

$$I_x = \iiint x^2 + y^2 dm \; ; I_{xy} = \iiint xy \; dm \quad (35)$$

$$I_{yz} = \iiint yz \; dm \; ; I_{xz} = \iiint xz \; dm \quad (36)$$

The moment applied on the aircraft in the x, y and z axis are denotes as L, M and N respectively. The set of moment equations are given by:

$$I_x\dot{p} + I_{xz}\dot{r} + (I_z - I_y)qr + I_{xz}qp = L \quad (37)$$

$$I_y\dot{q} + (I_x - I_x)pr + I_{xz}(r^2 - p^2) = M \quad (38)$$

$$I_z\dot{r} + I_{xz}\dot{p} + (I_y - I_x)qp - I_{xz}qr = N \quad (39)$$

The overall assumptions associated with the ADM are a rigid body RPAS, rigidly mounted aircraft engine on the vehicle body, the aircraft mass located in the aircraft centre of gravity and hence the mass is varying only as a result of fuel consumption, neglecting the wind effects, no sideslip, uniform gravity and the geodetic coordinate system of reference is World Geodetic System of year 1984 (WGS 84). The uncertainties in the aerodynamic parameters the primary source of errors in the model resulting from the use of the ADM. The accuracy of these parameters depends on the source of the data, which are theoretical computations, wind tunnel experiments and flight tests. The aerodynamic parameters can also be estimated using an adaptive UKF. To alleviate the effect of uncertainties, accurate data is used for modelling purposes. The covariance matrix describes the effect of uncertainties in the estimation of the states as a function of time.

B. Manoeuvre Recognition Algorithm

In several practical applications, the use of 3-DoF dynamics models is preferred. Indeed, to effectively use a Six Degree of Freedom (6-DoF) model a large amount of coefficients is needed and these are not always easy to determine or find. Therefore, a Manoeuvre Recognition Algorithm (MRA) is implemented that allows a reliable use of the aircraft 3-DoF dynamics model in all relevant flight phases. The inputs needed to perform this analysis are mainly attitude angles, altitude, angular rates, data about flaps and landing-gear states. Attitude angles and angular rates can be provided by VBS measurements, altitude by radio-altimeter and data about flaps and landing-gear can be provided from their respective actuators.

III. NAVIGATION AND GUIDANCE SYSTEM ARCHITECTURE

The two multi-sensor integrated NGS architectures compared are the EKF based VBN-IMU-GNSS-ADM (E-VIGA) and the UKF based system (U-VIGA). The U-VIGA architecture is illustrated in Fig. 7.

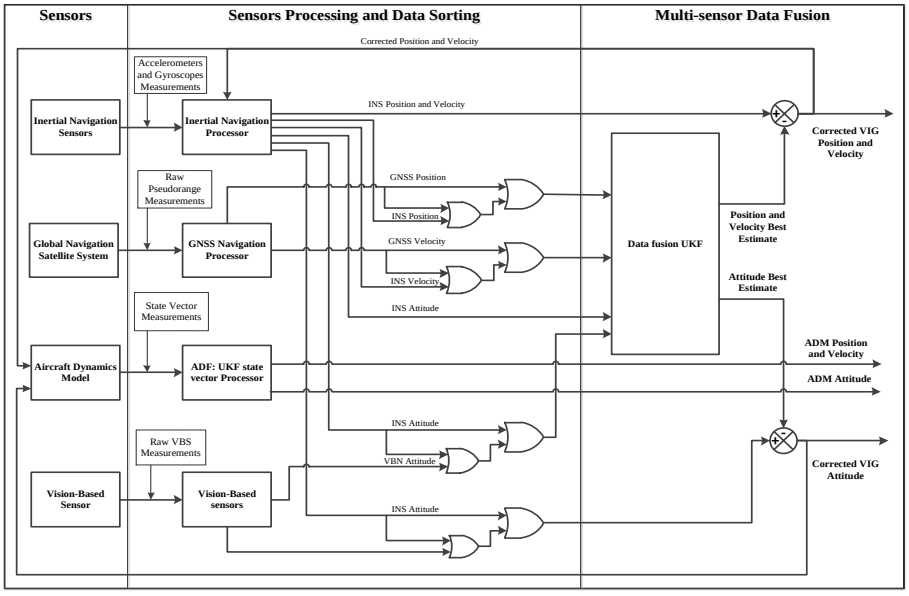

Fig. 7. U-VIGA architecture.

The E-VIGA architecture [6] uses VBN at 20 Hz and Global Positioning System (GPS) at 1 Hz to augment the MEMS-IMU running at 100 Hz. This architecture includes ADM (computations performed at 100 Hz) to provide attitude channel augmentation. The sensor measurements are handled by a sensor processing and data sorting block. The data sorting algorithm is based on Boolean decision logics, which allow automatic selection of the sensor data based on pre-defined priority criteria. The sorted data is then fed to an EKF to obtain the best estimate values. The INS position and velocity are compared with the GPS position and velocity to form the measurement input of the data fusion block containing the EKF. The attitude data provided by the ADM and the INS are compared to feed the EKF at 100 Hz, and the attitude data provided by the VBN sensors and INS are compared at 20 Hz and form the inputs to the EKF. The EKF provides estimates of Position, Velocity and Attitude (PVA) errors, which are then removed from the sensor measurements to obtain the corrected PVA states. An additional UKF is also used to pre-process the ADM navigation solution. The pre-filtering of the ADM virtual sensor measurements aids in achieving reduction of the overall position and attitude error budget and allows a considerable reduction in the ADM re-initialisation time. PVA measurements are obtained as state vectors from both the centralised UKF and ADM/UKF.

IV. Simulation Case Study

A detailed case study was performed in a high dynamics PAS environment, employing a 6-DoF model of the AEROSONDE RPAS as the reference ADM. The corresponding E-VIGA and U-VIGA integrated navigation modes were simulated using MATLAB™ in an appropriate sequence of flight manoeuvres representative of the AEROSONDE RPAS operational flight envelope. The duration of the simulation is 950 seconds covering eight flight legs (i.e., take off, straight climb, right climb helix, straight and level cruise, loiter, straight and level cruise, left descent helix, final straight approach) from starting point to destination. The 3D trajectory plot of the flight profiles of the AEROSONDE RPAS is illustrated in Fig. 8.

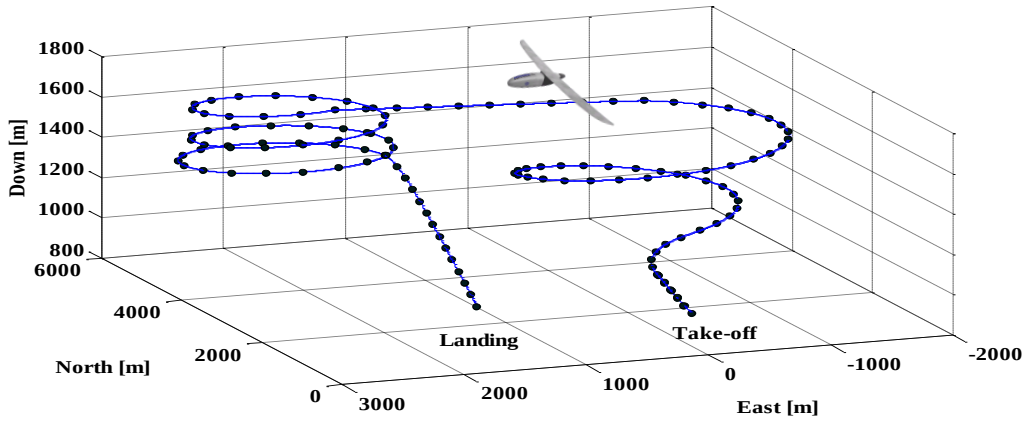

Fig. 8. 3D trajectory plot of RPAS flight profile.

The best estimates of position, velocity and attitude for the two NGS architectures are obtained and the associated error statistics are calculated. Tables 1 and 2 list the position and attitude error statistics of the two NGS architectures respectively. The E-VIGA NGS system is prone to rapid divergence and its optimal time for re-initialisation is in the order of 20 seconds. The U-VIGA NGS system shows considerable improvement in the horizontal and vertical positions. By applying an UKF to pre-filter the ADM measurements, the navigational solution is corrected and becomes suitable for an extended time of operation. Comparing with the E-VIGA solution, a significant improvement of the solution validity time is obtained with the U-VIGA system as shown in Table 3. In particular, the lateral position validity time before the solution exceeds the RNP 1 threshold in the climb phase is 227 sec and, in the final approach phase, the ADM solution exceeds the CAT I, CAT II and CAT III limits at 151 sec, 144 sec and 46 sec respectively.

Table 1: Position error statistics

NGS Architecture	North Position [m]		East Position [m]		Down Position [m]	
	μ	σ	μ	σ	μ	σ
E-VIGA	0.33	1.79	-0.48	1.81	-0.03	3.10
U-VIGA	0.37	1.78	-0.49	1.80	-1.40	3.10

Table 2: Attitude Error Statistics

NGS Architecture	Pitch (θ) [degrees]		Roll (ϕ) [degrees]		Heading (ψ) [degrees]	
	μ	σ	μ	σ	μ	σ
E-VIGA x10^-2	-0.52	2.67	-0.65	2.30	-0.56	0.29
U-VIGA x10^-2	-0.09	2.64	0.19	3.10	0.36	-0.16

TABLE 3: E-VIGA AND U-VIGA ADM LATERAL AND VERTICAL GUIDANCE VALIDITY TIMES

Accuracy threshold	ADM validity time [sec]			
	Lateral Position		Vertical Position	
	E-VIGA	U-VIGA	E-VIGA	U-VIGA
RNP 1	110	227	95	200
CAT I	107	151	62	116
CAT II	64	144	19	58
CAT III	41	46		

The vertical position validity time before the solution exceeds the RNP 1 threshold in the climb phase is 200 sec. Furthermore, CAT II and CAT III requirements were satisfied up to 58 sec and CAT I requirements up to 116 sec.

V. Human Machine Interface

In order to fulfill the requirements of RPAS coexistence with manned aircraft, a series of improvements are required specifically to increase reliability and situational awareness. In addition to requirements including DAA and enhanced navigation functions, one of the key improvements required is an adaptive HMI. The HMI among different RPAS designers and manufacturers varies a great deal in terms of the information presentation, and formats and functions. HMI consists of three main parts which are (1) operating elements, (2) displays, and (3) an inner structure. The inner structure encompasses hardware and software (i.e., electronic circuits and computer programmes). Displays show and transfer information about the machine to the user (for instance by means of graphical displays) and operating elements transfer information from the operator to the machine via for instance push buttons, switches, adjusting knobs, etc. The elements that contribute to an optimal HMI system design include the operational environment, human Perception, Cognition and Action (PCA) elements are illustrated in Fig. 9.

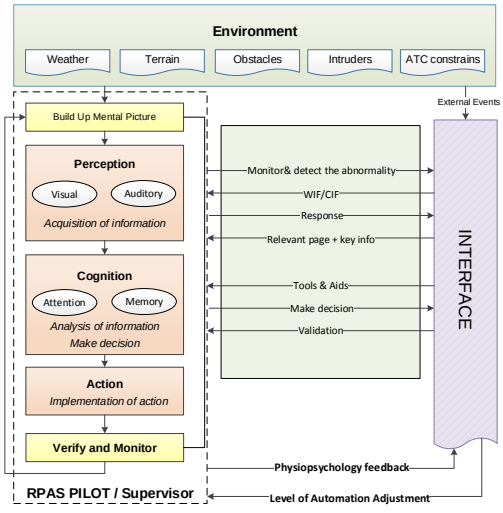

Fig. 9. HMI system design elements.

The core tasks of the RPAS pilot are listed below:

Mission Planning:

- Check all information related to a specific mission (i.e. take-off and landing data, operational area data, etc.).
- Create and validation the mission plan taking into account the fuel consumption optimization, targets/payloads characteristics, data link coverage, weather conditions and navigation aids.
- Perform a replanning as appropriate.

Surveillance:

- Monitor RPAS flight status.
- Monitor the system state (ensuring all systems are working properly).
- Monitor traffic status in the proximity of RPAS.
- Monitor weather status in the proximity of RPAS.
- Monitor compliance with the applicable Required Surveillance Performance (RSP).
- Make response to cautions and alerts.

Navigation:

- Monitor the RPAS navigation state.
- Select and tune applicable navigation modes.
- Monitor compliance with the applicable RNP requirements.
- Monitor and detect the obstacles/intruders.
- Track both low level and high level obstacles/intruders.
- Identify the potential risk of collision through predicting and evaluating the trajectory of intruders.
- Conduct criticality analysis for prioritizing, declaration and action determination.
- Create and execute the avoidance trajectory.

Communication and coordination:

- Contact with the remotely piloted aircraft by using LOS or BLOS datalink.
- Perform communications compliance with the applicable Required Communication Performance (RCP).
- Communicate with the relevant air traffic controllers.
- Communicate with the other airspace users.
- Communicate with civil authorities / local community.

Management:

- Process declaration of emergencies.
- Process a handover.

The ergonomics of the system has to cater for higher reliability and reduced workload of the remote pilot. Additionally, human factor elements are critical in RPAS due to the physical separation between the platform and GCS. Hence novel HMI solutions are developed in order to keep adequately the human operator inside the RPAS pilot control loop, providing a higher degree of automation, enhanced situational awareness and an affordable workload [35-37].

VI. CONCLUSION

The research activities performed to design a low-cost and low-weight/volume integrated NGS suitable for small-to-medium size RPAS applications were described. Various sensors were considered for the NGS design including GNSS and MEMS-IMU, with augmentation from ADM and VBN sensors. A low-cost and low-weight/volume integrated NGS architectures was introduced. The UKF based U-VIGA system. The U-VIGA system employs an UKF for pre-filtering the ADM attitude solution and thus increases the ADM solution validity time. Compared to the E-VIGA system used in previouse research, the U-VIGA system showed an improvement of accuracy in the position and attitude measurements in addition to an increased ADM validity time. Furthermore, the performance of the UKF processing attitude channel data from the ADM was validated with a Monte Carlo simulation. Additionally, the integration schemes achieved horizontal/vertical position accuracies in line with ICAO requirements. Future research will address uncertainty analysis and possible synergies of the U-VIGA architecture with GNSS avionics based integrity augmentation systems. The Mission Management System integration in Unmanned Aircraft System (UAS) improves operational capabilities in terms of navigation, planning, communication management and 4D trajectory control, taking into account the problems of current manned Flight Management System (FMS) HMI.

REFERENCES

1. R. Sabatini, S. Ramasamy, F. Cappello, and A. Gardi, "RPAS Navigation and Guidance Systems based on GNSS and other Low-Cost Sensors," Fourth Australasian Unmanned Systems Conference 2014 (ACUS 2014), Melbourne, Australia. DOI: 10.13140/2.1.3792.8008
2. A.S. Laliberte, A Rango, and J.E. Herrick, "Unmanned Aerial Vehicles for Rangeland Mapping and Monitoring: A Comparison of Two Systems", Proceedings of the ASPRS Annual Conference, Tampa, Florida, USA, 2007.
3. Doc 9750 – Global Air Navigation Capacity & Efficiency Plan 2013-2028, The International Civil Aviation Organization (ICAO), 4th edition, Montreal, Canada, 2014.
4. A. Gardi, R. Sabatini, S. Ramasamy, and T. Kistan, "Real-Time Trajectory Optimisation Models for Next Generation Air Traffic Management Systems," Applied Mechanics and Materials, vol. 629, Trans Tech Publications, Switzerland, pp. 327-332, 2014. DOI: 10.4028/www.scientific.net/AMM.629.327
5. M. Guoqiang, S. Drake, and B.D. Anderson, "Design of an Extended Kalman Filter for UAV Localization," IEEE Conference on Information, Decision and Control (IDC'07), Adelaide, Australia, 2007.
6. J. Hannuksela, "Facial Feature Based Head Tracking and Pose Estimation," Department of Electrical and Information Engineering, University of Oulu, Finland, 2003.
7. Y. Hua, and G. Welch, "Model-based 3D Object Tracking Using an Extended-extended Kalman Filter and Graphics Rendered Measurements," IEEE Computer Vision for Interactive and Intelligent Environment, Lexington, Kentucky, 2005.
8. N. Ingemars, "A Feature based Face Tracker using Extended Kalman Filtering," Department of Electrical Engineering, Linköpings Universitet, Sweden, 2007.
9. International Civil Aviation Organisation (ICAO), Doc 9750 for Global Air Navigation Plan for CNS/ATM Systems, 2nd edition, Montréal, Quebec, Canada, 2002.
10. M.T. Degarmo, "Issues Concerning Integration of Unmanned Aerial Vehicles in Civil Airspace," The MITRE Corporation Center for Advanced Aviation System Development, 2004.
11. Federal Aviation Administration (FAA), AC 120-29A. Advisory Circular - Criteria for Approval of Category I and Category II Weather Minima for Approach, U.S. Department of Transportation, 2012.
12. D. Jiang, et al., "Advances in Multi-Sensor Data Fusion: Algorithms and Applications", Journal of Sensors, Vol. 9, Issue. 10, 2009, pp. 7771-7784.
13. J.H. Wang, and Y. Gao, "The Aiding of MEMS INS/GPS Integration Using Artificial Intelligence for Land Vehicle Navigation", IAENG International Journal of Computer Science, vol. 33, issue 1, 2011.
14. T.N. Ranjan, A. Nherakkol, and G. Navelkar "Navigation of Autonomous Underwater Vehicle Using Extended Kalman Filter", 13th FIRA RobotWorld Congress, FIRA 2010 Bangalore, India, September, 2010.
15. H. Kondo, T. Maki, T. Ura, and T. Sakamaki, "AUV Navigation based on Multi-Sensor Fusion For Breakwater Observation," ISARC2006 International Symposium on Automation and Robotics in Construction, 2006.
16. R.v.d., Merwe, and E.A. Wan, "The Square-Root Unscented Kalman Filter for State and Parameter-Estimation", Proceedings of the IEEE International Conference on Acoustics, Speech, and Signal Processing (ICASSP'01), vol. 6, 2001.
17. H. Pesonen and R. Piche, "Cubature-based Kalman Filters for Positioning" 7th Workshop on Positioning, Navigation and Communication (WPNC), 2010.
18. M. Norgaard, N. Poulsen, and O. Ravn., "New Developments in State Estimation for Nonlinear

Systems", Automatica, vol. 36, no. 11, pp. 1627–1638, November 2000.
19. Malinowski, M. and Kwiecień, J., "Study of The Effectiveness of Different Kalman Filtering Methods and Smoothers in Object Tracking Based on Simulation Tests", Reports on Geodesy and Geoinformatics, vol. 97, pp. 1-22, 2014. DOI: 10.2478/rgg-2014-0008
20. F. Gustafsson, F. Gunnarsson, N. Bergman, U. Forssell, J. Jansson, R. Karlsson, and P.J. Nordlund, "Particle Filters for Positioning, Navigation, and Tracking" IEEE Transactions on Signal Processing, vol. 50, no. 2, February 2002.
21. R. Kandepu, B. Foss, and L. Imsland, "Applying the Unscented Kalman filter for Nonlinear State Estimation", Journal of Process Control, vol. 18, issue 7/8, 2008.
22. J. Julier, and J.K. Uhlmann, "A new extension of the Kalman filter to nonlinear systems," in Proceedings of AeroSense: The11th International Symposium on Aerospace/Defence Sensing, Simulation and Controls, 1997, pp. 182–193.
23. E.A. Wan, and R.v.d. Merwe, "The Unscented Kalman Filter for Nonlinear Estimation", Proceedings of Symposium 2000 on Adaptive Systems for Signal Processing, Communication and Control (AS-SPCC), Lake Louise, Alberta, Canada, 2000.
24. R. Sabatini, F. Cappello, S. Ramasamy, A. Gardi, and R. Clothier, "An Innovative Navigation and Guidance System for Small Unmanned Aircraft using Low-Cost Sensors," In press, Aircraft Engineering and Aerospace Technology, vol. 87, Emerald Publishing Group Ltd., 2015 (In press).
25. R. Sabatini, C. Bartel, A. Kaharkar, T. Shaid, and S. Ramasamy, "Navigation and Guidance System Architectures for Small Unmanned Aircraft Applications," International Journal of Mechanical, Aerospace, Industrial and Mechatronics Engineering, vol. 8, no. 4, pp. 733-752, International Science Index, April 2014.
26. R. Sabatini, L. Rodriguez, A. Kaharkar, C. Bartel, T. Shaid, and D. Zammit-Mangion, "Low-Cost Navigation and Guidance Systems for Unmanned Aerial Vehicles – Part 2: Attitude Determination and Control," Annual of Navigation, vol. 20, pp. 97-126, November 2013. DOI: 10.2478/aon-2013-0008
27. R. Sabatini, S. Ramasamy, A. Gardi and L. Rodriguez Salazar, "Low-cost Sensors Data Fusion for Small Size Unmanned Aerial Vehicles Navigation and Guidance." International Journal of Unmanned Systems Engineering, Vol. 1, No. 3, pp. 16-47, August 2013. DOI: 10.14323/ijuseng.2013.11
28. R. Sabatini, M.A. Richardson, C. Bartel, T. Shaid, and S. Ramasamy, "A Low-cost Vision Based Navigation System for Small Size Unmanned Aerial Vehicle Applications." Journal of Aeronautics and Aerospace Engineering, vol. 2, no. 3, May 2013. DOI: 10.4172/2168-9792.1000110
29. R. Sabatini, C. Bartel, A. Kaharkar, and T. Shaid, "Low-cost Vision Sensors and Integrated Systems for Unmanned Aerial Vehicle Navigation and Guidance," ARPN Journal of Systems and Software, ISSN: 2222-9833, vol. 2, issue 11, pp. 323-349, December 2012.
30. R. Sabatini, C. Bartel, A. Kaharkar, T. Shaid, L. Rodriguez, D. Zammit-Mangion, and H. Jia, "Low-Cost Navigation and Guidance Systems for Unmanned Aerial Vehicles – Part 1: Vision-Based and Integrated Sensors," Annual of Navigation, vol. 19, issue 2, pp. 71-98, December 2012. DOI: 10.2478/v10367-012-0019-3
31. M. Omerbashich, "Integrated INS/GPS Navigation from a Popular Perspective", Journal of Air Transportation, vol. 7, no. 1, 2002.
32. T.S. Bruggemann, "Investigation of MEMS Inertial Sensors and Aircraft Dynamics Model in Global Positioning System Integrity Monitoring for Approaches with Vertical Guidance", Dissertation, Queensland University of Technology, 2009.
33. L. Cork, "Aircraft Dynamics Navigation for Unmanned Aerial Vehicles", Dissertation, Queensland University of Technology, 2014.
34. J. Zhou, S. Knedlik, E. Edwan, and O. Loffeld, "Low-Cost INS/GPS with Nonlinear Filtering Methods", 13th IEEE Information Fusion (FUSION) conference, 2010.
35. R. Parasuraman, "Designing Automation for Human Use: Empirical Studies and Quantitative Models", Ergonomics, 43, pp. 931-951, 2000.
36. R.W. Proctor, and T. Van Zandt, "Human Factors in Simple and Complex Systems", CRC press, 2008.
37. D.C. Wickens, J. Lee, Y. Liu, and G. S. Becker, "An Introduction to Human Factors Engineering", USA, Pearson Education, Inc., 2004.